Direct conversion of syngas to aromatics with two step C-C coupling over MnZr/H-ZSM-5 bifunctional catalyst of OX-ZEO strategy

Shiyu Liu[1], Qiuyun Huang[1], Ijaz Ul Haq[1], Zixu Yang[1], Weihua Shen[1,*] and Yunjin Fang[1,*]

1. State Key Laboratory of Chemical Engineering, School of Chemical Engineering, East China University of Science and Technology, Shanghai 200237, China

*Corresponding Author

Email: whshen@ecust.edu.cn(Prof. Shen); yjfang@ecust.edu.cn(Prof. Fang)

Tel: +86-21-64252829

Content

1. Characterization results

Table S1 Composites of fresh oxides and zeolites by XRF

Entry	Sample	Mn (mol%)	Zr (mol%)	Si (mol%)	Al (mol%)	Si/Al ratio
1	MnO_X	100	0			
2	8Mn2Zr	78.89	21.11			
3	6Mn4Zr	59.35	40.65		/	
4	4Mn6Zr	36.50	63.50			
5	2Mn8Zr	19.73	80.27			
6	ZrO_2	0	100			
7	H-ZSM-5(30)			97.07%	2.93%	33.12
8	H-ZSM-5(60)		/	98.32%	1.68%	58.52
9	H-ZSM-5(120)			99.16%	0.84%	118.05
10	H-ZSM-5(200)			99.47%	0.53%	187.68

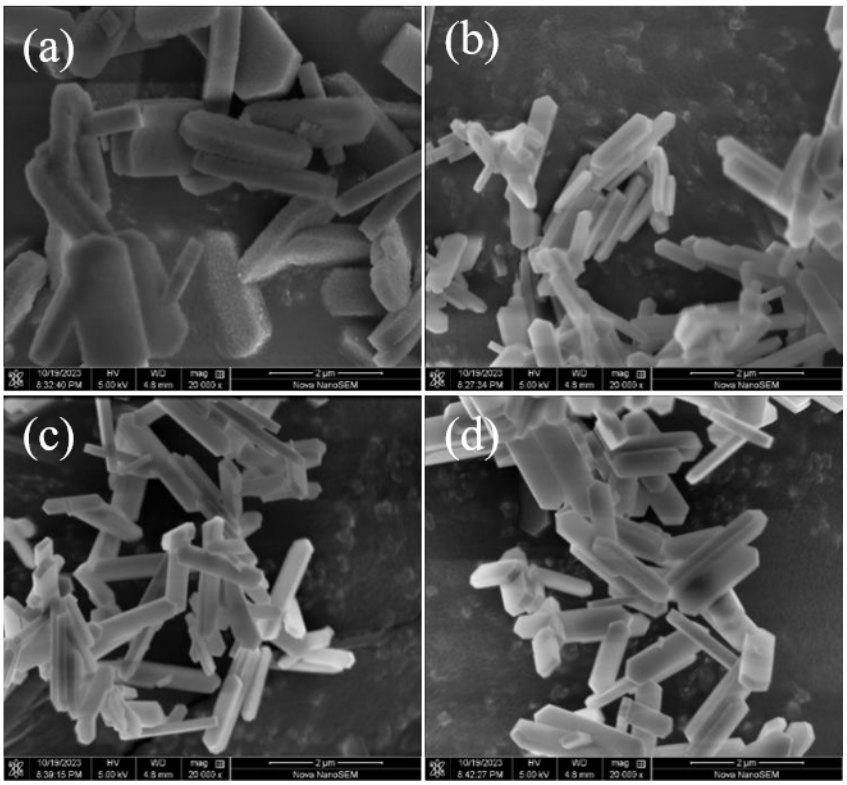

Figure S1 SEM figures of HZSM-5 with different Si/Al ratio (a) 30; (b) 60; (c) 120; (d) 200.

Table S2 Crystal size (nm) of oxides calculated by Scherrer equation.

Sample	Mn_2O_3	MnO	*m*-ZrO_2	*t*-ZrO_2	$Mn_{0.2}Zr_{0.8}O_{1.8}$
MnO_X*	32.9	/	/	/	/
8Mn2Zr*	28.6	/	/	/	10.4
6Mn4Zr*	27.0	/	/	/	9.9
4Mn6Zr*	26.3	/	/	/	9.6
2Mn8Zr*	/	/	/	/	12.3
ZrO_2*	/	/	11.0	15.9	/
MnO_X**	/	44.7	/	/	/
8Mn2Zr**	/	29.6	/	/	10.8
6Mn4Zr**	/	29	/	/	10
4Mn6Zr**	/	27.0	/	/	10.4
2Mn8Zr**	/	/	/	/	13.5
ZrO_2**	/	/	13.4	/	/

** Obtained from the fresh oxide patterns (figure 1b).

* Obtained from the spent bifunctional catalyst patterns (figure 1d).

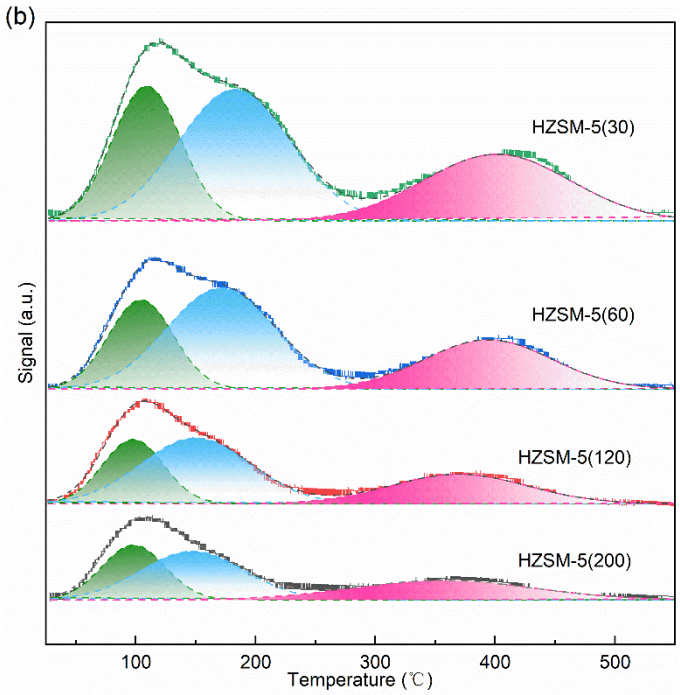

Figure S2 NH_3-TPD profile of H-ZSM-5 with different Si/Al ratio.

Table S3 Quantification of acid density over HZSM-5 with different Si/Al ratio (from figure S2)

Si/Al ratio	Acid sites distribution			Total acid sites
	Weak acid sites	Medium strong acid sites	Strong acid sites	μmol/g
30	63.97%	27.93%	8.09%	142.04
60	62.26%	29.63%	8.11%	73.45
120	62.41%	29.71%	7.88%	42.54
200	64.85%	27.24%	7.91%	35.76

Table S4 Quantification oxides O 1s orbit with different composition (from figure 2b)

Oxides	Lattice O (O_L)	Vacancy O(O_V)	Chemi-sorbed O(O_C)
MnO_X	70.77%	13.55%	15.68%
8Mn2Zr	68.57%	19.32%	12.11%
6Mn4Zr	71.96%	20.38%	7.66%
4Mn6Zr	62.78%	21.00%	16.23%
2Mn8Zr	58.34%	28.12%	13.54%
ZrO_2	66.31%	22.82%	10.87%

Table S5 Quantification oxides Mn 2p orbit with different composition (from figure 2c)

Oxides	Mn^{2+}	Mn^{3+}
MnO_X	37.08%	62.92%
8Mn2Zr	46.05%	53.95%
6Mn4Zr	51.46%	48.54%
4Mn6Zr	54.29%	45.71%
2Mn8Zr	59.30%	40.70%

Table S6 Analysis of in-situ diffuse reflectance infrared spectroscopy (DRIFTS) adsorption peaks

Mode	Wavenumber (cm^{-1})	From species	Reference wavenumber (cm^{-1})	Reference
ν(OH)	3754	Terminal surface -OH	3770	[1]
ν(OH)	3687	Methanol	/	/
ν(OH)	3658	Bridged surface -OH	3668	[1]
ν(OH)	3582	Ethanol	3000-3700	[2]
$\nu_{as}(CH_3)$	3009	Methyl	3005	[3]
$\nu_{as}(CH_3)$	2973	Ethoxyl	2970	[2, 4]
$\delta(CH) + \nu_{as}(OCO)$	2959	Formate	2965	[5]
$\nu_{as}(CH_3)$	2929	Methoxyl	2930/2922/2923	[2, 3, 5]
$\nu_{as}(CH_2)$	2877	Ethoxyl	2875	[2]
ν(CH)	2856	Formate	2855	[4]
$\nu_s(CH_3)$	2814	Methanol	2820	[3, 5]
$\delta(CH) + \nu_s(OCO)$	2739	Formate	2751	[5]
$\delta(CH) + \nu_s(OCO)$	2713	Formate	2737	[5]
ν(C=O)	1748	Formyl	1756	[6]
ν(C=O)	1675/1698	Alkyl-aldehyde	1650-1700	[2]
$\nu_{as}(OCO)$	1600	Formate	1593	[7]
$\nu_{as}(OCO)$	1583	Formate	1581/1560	[5]
$\nu_{as}(OCO)$	1566	Carbonate	1563	[7]
$\nu_{as}(OCO)$	1549	Acetate	1547/1545	[2]
$\nu_s(OCO)$	1437	Carbonate	1426	[7]
ν(terminal-CO)	1142	Methoxyl	1149/1154	[5, 8]
ν(CO)	1066	Ethoxyl	1065	[2]
v(bridged-CO)	1042	Methoxyl	1047/1043/1052	[5, 8]
ν(CO)	1017	Methoxyl	/	/

The peak at 3687 cm^{-1} appeared only at H_2 abundant environment; moreover, the strength was relative strong, thus we ascribed this peak as the adsorption of ν(OH) of hydrogen-bonded methanol which was similar with reference [2]. The peak at 1017 cm^{-1} should be the adsorption peak of ν(CO), as it appeared and increased during CO adsorption, it was supposed relative to methoxyl groups with higher coordination.

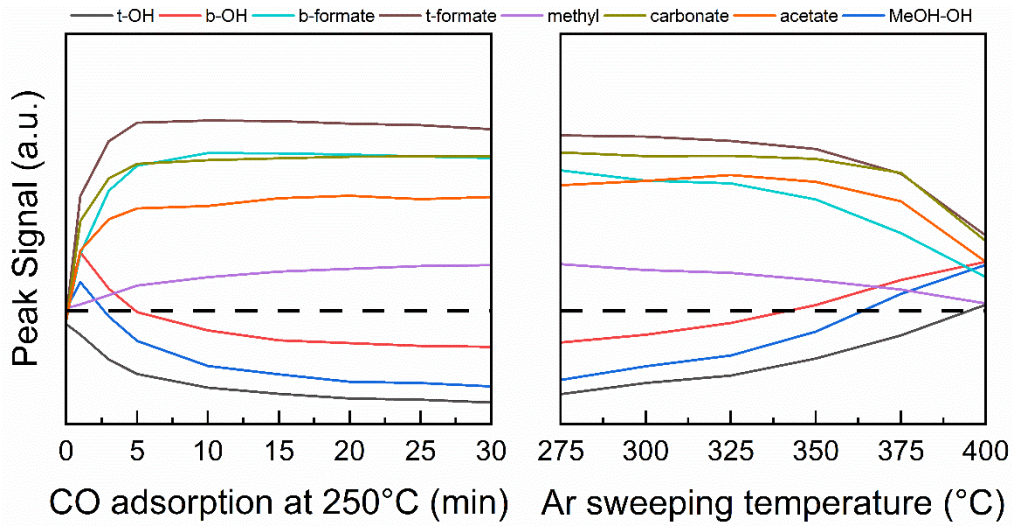

Figure S3. Peak signal of surface species in Figure 3(a).

t-OH (3754 cm^{-1}, ν(OH)), b-OH (3658 cm^{-1}, ν(OH)), b-formate (1600 cm^{-1}, ν_{as}(OCO)), t-formate (1583 cm^{-1}, ν_{as}(OCO)), methyl (3009 cm^{-1}, ν_{as}(CH)), carbonate (1566 cm^{-1}, ν_{as}(OCO)), acetate (1549 cm^{-1}, ν_{as}(OCO)), MeOH-OH (3687 cm^{-1}, ν(OH))

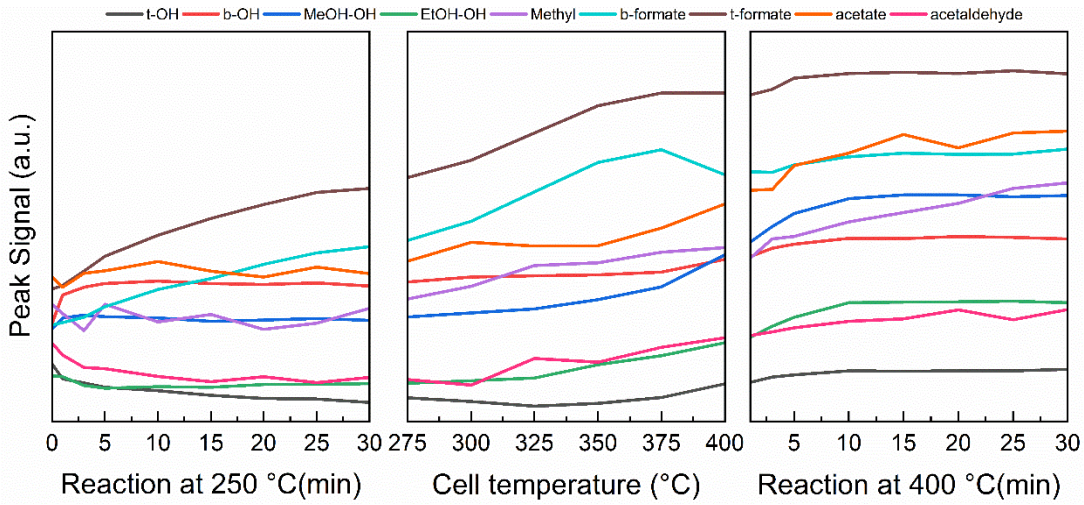

Figure S4. Peak signal of surface species in Figure 3(b).

*Methyl group signal was multiplied by 10 to enhance the trend

t-OH (3754 cm^{-1}, ν(OH)), b-OH (3658 cm^{-1}, ν(OH)), MeOH-OH (3687 cm^{-1}, ν(OH)), EtOH-OH (3582 cm^{-1}, ν(OH)), methyl (3009 cm^{-1}, ν_{as}(CH)), b-formate (1600 cm^{-1}, ν_{as}(OCO)), t-formate (1583 cm^{-1}, ν_{as}(OCO)), acetate (1549 cm^{-1}, ν_{as}(OCO)), acetaldehyde (1675 cm^{-1}, ν(C=O))

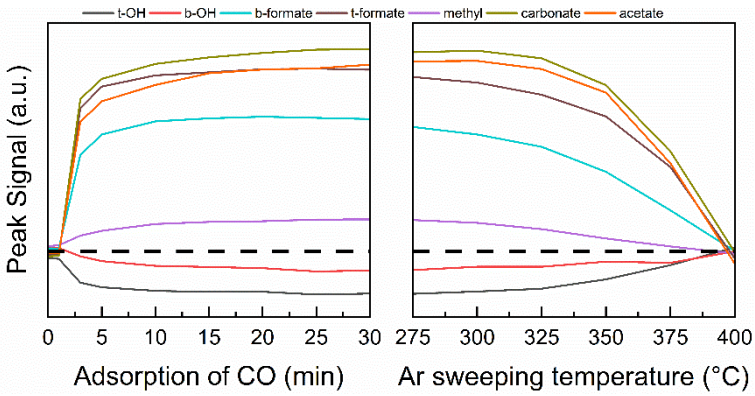

Figure S5. Peak signal of surface species in Figure 4(a).

t-OH (3754 cm^{-1}, ν(OH)), b-OH (3658 cm^{-1}, ν(OH)), b-formate (1600 cm^{-1}, ν_{as}(OCO)), t-formate (1583 cm^{-1}, ν_{as}(OCO)), methyl (3009 cm^{-1}, ν_{as}(CH)), carbonate (1566 cm^{-1}, ν_{as}(OCO)), acetate (1549 cm^{-1}, ν_{as}(OCO))

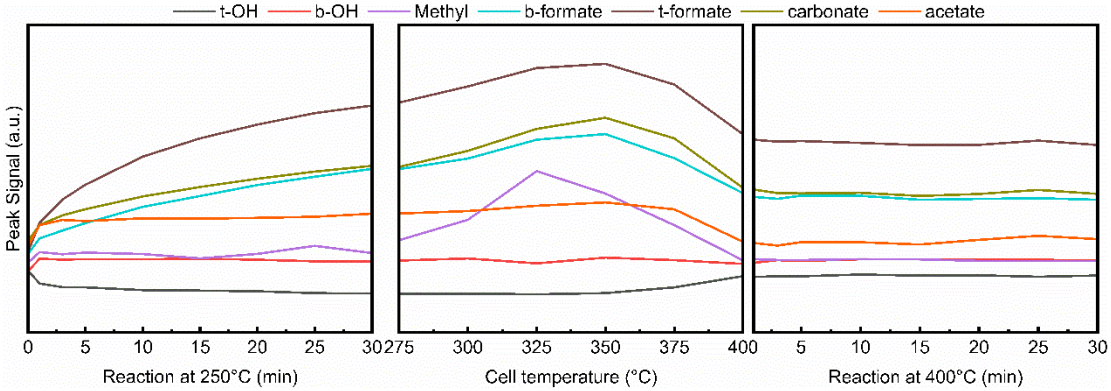

Figure S6. Peak signal of surface species in Figure 4(b).

*Methyl group signal was multiplied by 10 and acetate group signal was multiplied by 2 to enhance the trend

t-OH (3754 cm^{-1}, ν(OH)), b-OH (3658 cm^{-1}, ν(OH)), methyl (3009 cm^{-1}, ν_{as}(CH)), b-formate (1600 cm^{-1}, ν_{as}(OCO)), t-formate (1583 cm^{-1}, ν_{as}(OCO)), carbonate (1566 cm^{-1}, ν_{as}(OCO)), acetate (1549 cm^{-1}, ν_{as}(OCO))

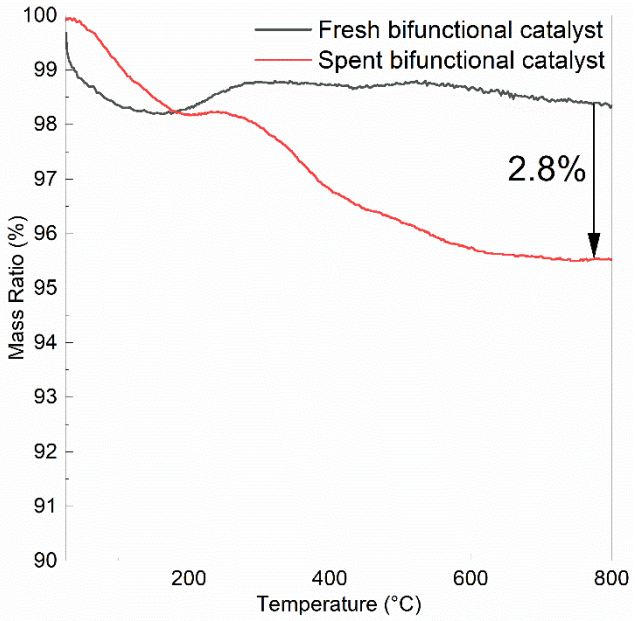

Figure S7 TG profile of bifunctional catalysts. (The fresh catalyst was pre-reduced with same procedure in catalyst evaluation section)

Table S7 Analysis of N_2 isothermal adsorption.

Sample	S_{BET} (m^2/g)[a]	S_{micro} (m^2/g)[b]	V_{total} (cm^3/g)[c]	V_{micro} (cm^3/g)[b]
Fresh bifunctional catalyst*	223.1	30.4	0.25	0.015
Spent bifunctional catalyst	210.8	21.9	0.24	0.011

[a] BET surface area.

[b] t-PLOT method for $D_P \leq 2$nm.

[c] Total pore volume, $P/P_0 = 0.99$.

* The fresh catalyst was pre-reduced with same procedure in catalyst evaluation section

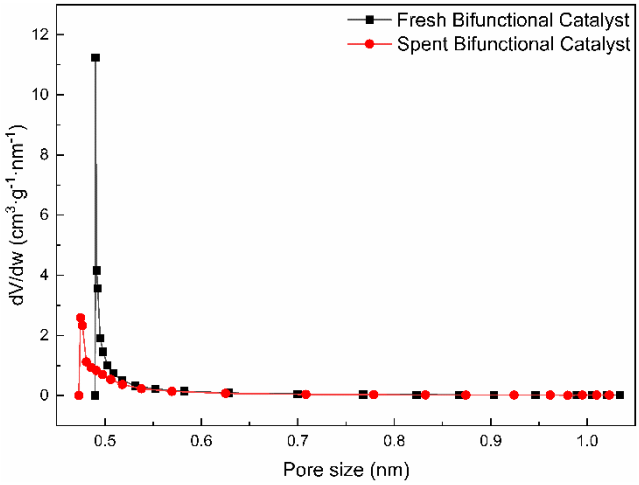

Figure S8 Pore size distribution of bifunctional catalysts from HK method. (The fresh catalyst was pre-reduced with same procedure in catalyst evaluation section)

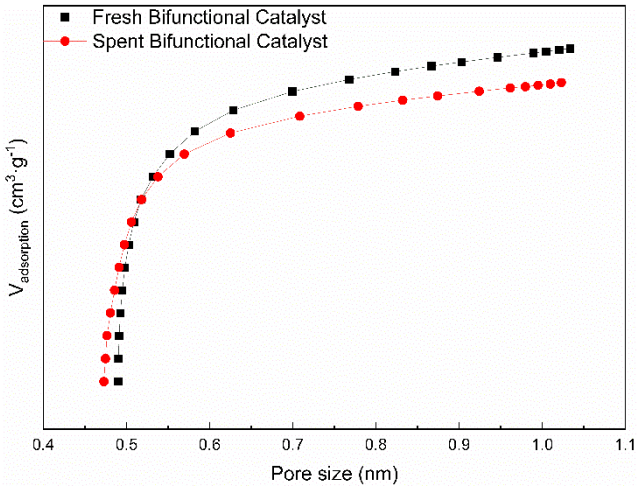

Figure S9 Cumulative Pore Volume ($cm^3 \cdot g^{-1}$) of bifunctional catalysts calculated from HK method. (The fresh catalyst was pre-reduced with same procedure in catalyst evaluation section)

2. Additional reaction results and products distribution

Table S8 reaction results of 6Mn4Zr/H-ZSM-5(60) with different intimacy

Mixing method	CO conversion	CO_2 selectivity	Hydrocarbon selectivity				
			Methane	C_2-C_4 paraffin	C_2-C_4 olefin	C_5^+	Aromatics
Layer mixing[a]	4.43%	30.53%	3.62%	25.65%	6.51%	19.30%	44.91%
Granule mixing	11.55%	46.08%	1.99%	26.58%	2.57%	7.85%	61.01%
Powder mixing	15.11%	43.86%	2.74%	3.56%	3.26%	5.67%	84.77%

Mass ratio of OX/ZEO = 1; reaction condition: 400 °C, 3 MPa, $H_2/CO = 2$, space velocity = 3000 $mL\cdot\cdot g_{cat}^{-1}\cdot h^{-1}$.

[a] oxides in the up-stream, oxides and zeolites were separated by quartz wool.

Table S9 reaction results of 6Mn4Zr/H-ZSM-5 with different Si/Al ratio

Si/Al ratio of H-ZSM-5	CO conversion	CO_2 selectivity	Hydrocarbon selectivity				
			Methane	C_2-C_4 paraffin	C_2-C_4 olefin	C_5^+	Aromatics
30	15.42%	39.47%	4.90%	9.79%	3.23%	4.03%	78.05%
60	15.11%	43.86%	2.74%	3.56%	3.26%	5.67%	84.77%
120	14.20%	42.73%	3.45%	4.46%	2.79%	7.46%	81.85%
200	14.04%	40.70%	3.85%	4.53%	3.56%	7.39%	80.67%

Mixing method: powder mixing; Mass ratio of OX/ZEO = 1; reaction condition: 400 °C, 3 MPa, $H_2/CO = 2$, space velocity = 3000 $mL\cdot\cdot g_{cat}^{-1}\cdot h^{-1}$.

Table S10 reaction results of 6Mn4Zr/H-ZSM-5(60) with different mass ratio

Mass ratio	CO conversion	CO_2 selectivity	Hydrocarbon selectivity				
			Methane	C_2-C_4 paraffin	C_2-C_4 olefin	C_5^+	Aromatics
1:2	12.44%	39.54%	6.94%	7.54%	1.38%	4.77%	79.37%
1:1	15.11%	43.86%	2.74%	3.56%	3.26%	5.67%	84.77%
1.5:1	14.61%	40.52%	5.07%	3.44%	2.03%	7.46%	81.99%
2:1	12.08%	41.05%	5.29%	2.97%	2.78%	9.71%	79.25%

Mixing method: powder mixing; reaction condition: 400 °C, 3 MPa, $H_2/CO = 2$, space velocity = 3000 $mL\cdot\cdot g_{cat}^{-1}\cdot h^{-1}$.

Table S11 reaction results of 6Mn4Zr/H-ZSM-5(60) at different reaction condition

Reaction Temperature (°C)	Reaction Pressure (MPa)	H_2/CO ratio	Space Velocity ($mL \cdot g_{cat} \cdot h^{-1}$)	CO conversion	CO_2 selectivity	Hydrocarbon selectivity				
						Methane	C_2-C_4 paraffin	C_2-C_4 olefin	C_5^+	Aromatics
350				6.58%	41.01%	2.76%	4.26%	1.47%	3.05%	88.46%
375				11.09%	40.55%	2.73%	4.05%	2.04%	5.08%	86.10%
400	3	2	3000	15.11%	43.86%	2.74%	4.56%	2.26%	5.67%	84.77%
425				19.08%	42.44%	6.69%	8.23%	5.56%	5.13%	74.39%
450				23.51%	40.66%	15.39%	15.00%	8.86%	6.22%	54.53%
	1			6.28%	41.52%	2.57%	11.71%	3.65%	11.28%	70.79%
	2			10.99%	41.42%	4.21%	4.42%	3.60%	6.29%	81.47%
400	3	2	3000	15.11%	43.86%	2.74%	4.56%	2.26%	5.67%	84.77%
	4			22.27%	39.60%	11.53%	6.60%	2.26%	5.57%	74.04%
	5			25.15%	41.57%	12.07%	6.93%	1.85%	6.62%	72.53%
		1		12.86%	44.10%	1.89%	4.96%	1.07%	6.23%	85.85%
		2		15.11%	43.86%	2.74%	4.56%	2.26%	5.67%	84.77%
400	3		3000							
		3		18.52%	36.28%	3.22%	11.71%	1.49%	6.73%	76.85%
		4		19.84%	33.78%	3.85%	14.21%	1.48%	7.65%	72.81%
			600	36.36%	41.86%	3.15%	5.02%	2.38%	2.21%	87.24%
			1200	26.17%	42.09%	2.72%	4.45%	2.56%	2.76%	87.51%
400	3	2	1800	21.41%	42.56%	2.55%	4.46%	2.76%	2.86%	87.37%
			2400	18.21%	42.10%	2.45%	4.85%	2.99%	3.61%	86.10%
			3000	15.11%	43.86%	2.74%	3.56%	3.26%	5.67%	84.77%

Mixing method: powder mixing; Mass ratio of OX/ZEO = 1.

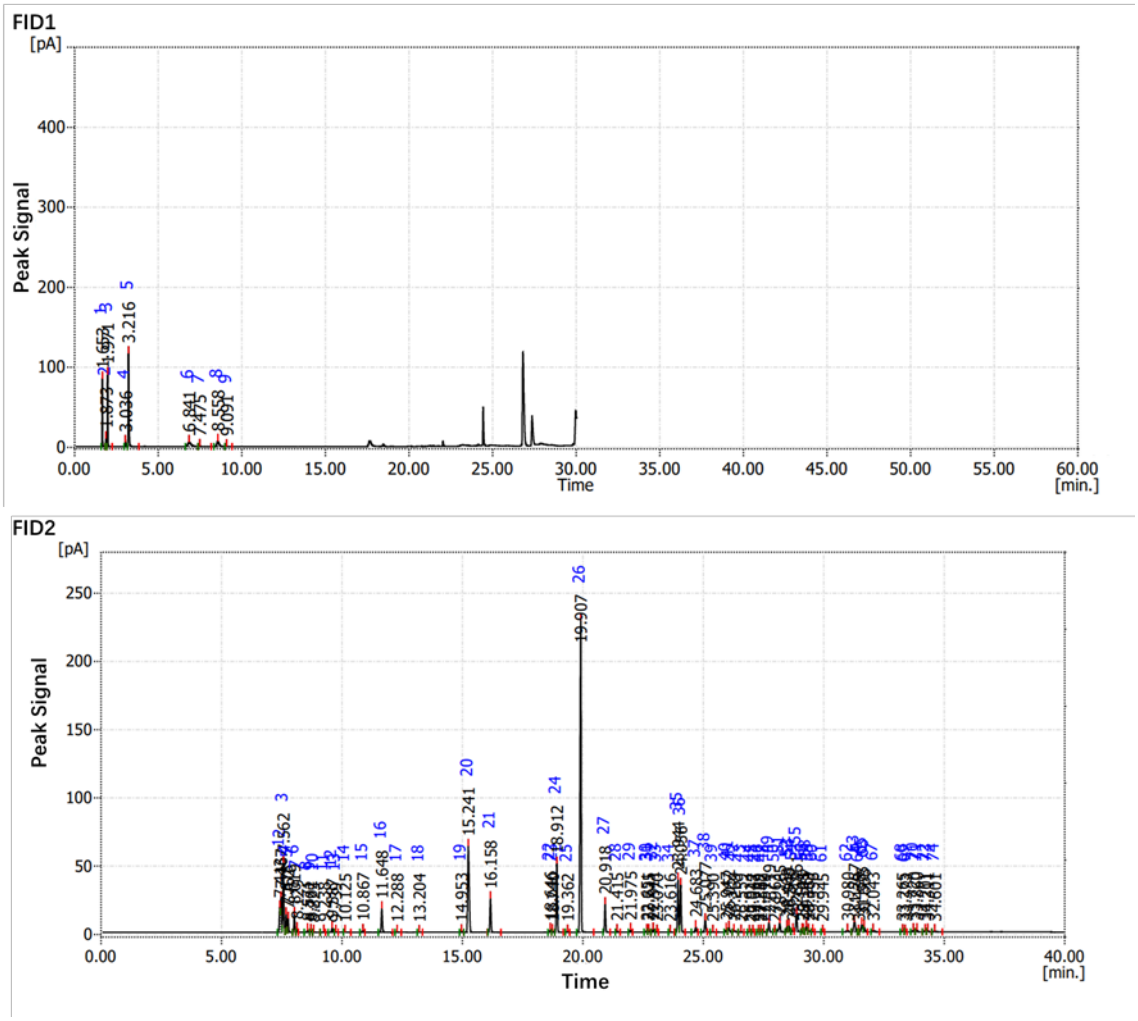

Figure S10 GC profile of organic products (obtained from t = 31 h in stability evaluation).

Qualitative analysis of peaks in figure S10:

For FID1, the peak from 1 to 9 is methane, ethylene, ethane, propylene, propane, n-butane, butene, i-butane, butene

For FID2, the aromatics product peaks were listed here, peak 12 is benzene (it was nearly covered by other peaks); peak 16 is toluene; Peak 20 is mixing peak of p-xylene and m-xylene; peak 21 is o-xylene; peak 24 is 1,3,5-trimethylbenzene; peak 26 is 1,2,4-trimethylbenzene; peak 27 is 1,2,3-trimethylbenzene; peak 35 and 36 is tetramethylbenzene; peak 37+ is heavy aromatics including naphthalene and methylnaphthalene etc.

Table S12 detailed products distribution (calculated from GC profile of figure S10)

Light Hydrocarbons	Methane	Ethylene	Ethane	Propylene	Propane	Butane	butene	
	2.33%	0.30%	2.70%	0.19%	5.61%	2.33%	0.08%	
C_5^+ Hydrocarbons	C_5-C_6 non-aromatics	C_7 non-aromatics	C_8 non-aromatics	Benzene	Toluene	Xylene	trimethylbenzene	C_{10}^+ aromatics
	1.99%	0.27%	1.28%	0.37% (0.45%)	2.45% (2.95%)	14.79% (17.84%)	40.54% (48.89%)	24.77% (29.87%)

The aromatics distribution was listed in brackets.

3. Scheme for reaction mechanism over oxides

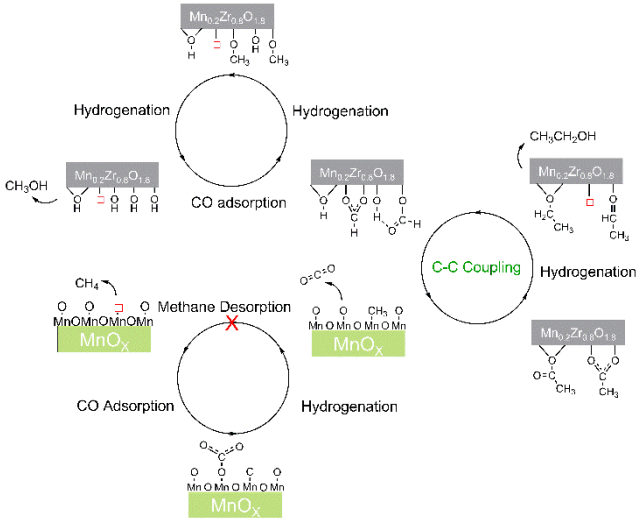

Scheme S1. Reaction mechanism of syngas conversion over 6Mn4Zr alone.

Reference

1. Ouyang, F., et al., *Isotope-exchange reaction between hydrogen molecules and surface hydroxy groups on bare and modified ZrO2.* Journal of the Chemical Society, Faraday Transactions, 1996. **92**(22): p. 4491-4495.
2. Ochoa, J.V., et al., *In Situ DRIFTS-MS Study of the Anaerobic Oxidation of Ethanol over Spinel Mixed Oxides.* The Journal of Physical Chemistry C, 2013. **117**(45): p. 23908-23918.
3. Wang, X., et al., *Effects of surface acid–base properties of ZrO2 on the direct synthesis of DMC from CO2 and methanol: A combined DFT and experimental study.* Chemical Engineering Science, 2021. **229**: p. 116018.
4. Kalered, E., et al., *Infrared Fingerprints of the CO2 Conversion into Methanol at Cu(s)/ZrO2(s): An Experimental and Theoretical Study.* ChemCatChem, 2023. **16**(3): p. e202300886.
5. Kattel, S., et al., *Optimizing Binding Energies of Key Intermediates for CO2 Hydrogenation to Methanol over Oxide-Supported Copper.* J Am Chem Soc, 2016. **138**(38): p. 12440-50.
6. Li, J., et al., *Hollow cavity engineering of MOFs-derived hierarchical MnOx structure for highly efficient photothermal degradation of ethyl acetate under light irradiation.* Chemical Engineering Journal, 2023. **464**: p. 142412.
7. Qian, W., et al., *In Situ DRIFTS Study of Homologous Reaction of Methanol and Higher Alcohols Synthesis over Mn Promoted Cu–Fe Catalysts.* Industrial & Engineering Chemistry Research, 2019. **58**(16): p. 6288-6297.
8. Ouyang, F., et al., *Site Conversion of Methoxy Species on ZrO2.* The Journal of Physical Chemistry B, 1997. **101**(25): p. 4867-4869.